

Achieving Linear α -Macro-olefins in Ethylene Polymerization through Precisely Tuned Bis(imino)pyridylcobalt Precatalysts with Steric and Electronic Parameters

Kainat Fatima Tahir, Yanping Ma,* Qaiser Mahmood,* Geng Ren, Areej Khalid, Yizhou Wang, Song Zou, Tongling Liang, and Wen-Hua Sun*



Cite This: *Precis. Chem.* 2024, 2, 655–668



Read Online

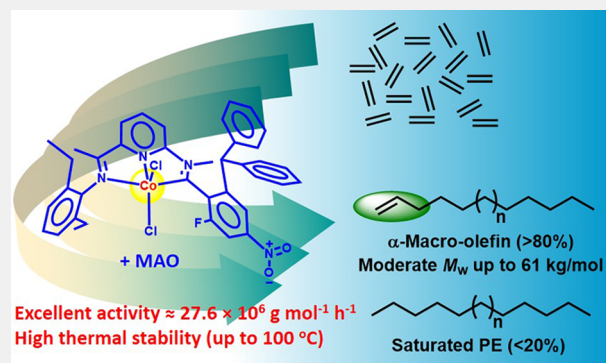
ACCESS |

Metrics & More

Article Recommendations

Supporting Information

ABSTRACT: Synthesis of functional polyethylene from ethylene alone is tricky and heavily dependent on both the type and structure of the precatalyst and the choice of cocatalyst used in the polymerization. In the present study, a series of cobalt precatalysts was prepared and investigated for ethylene polymerization under various conditions. By incorporation of strong electron-withdrawing groups (F and NO₂) and a steric component (benzhydryl) into the parent bis(imino)pyridine ligand, the catalytic performance of these precatalysts was optimized. On activation with MAO or MMAO, these precatalysts with relatively open structure achieved unprecedented ethylene polymerization rates at 60 °C (up to $27.6 \times 10^6 \text{ g mol}^{-1} \text{ h}^{-1}$) and remained effective at temperatures up to 100 °C. Chain growth reactions were moderate, resulting in polyethylene with molecular weights up to 61.0 kg/mol and broad bimodal dispersity index. High crystallinity and melt temperature indicated a strictly linear microstructure, as further confirmed by high-temperature ¹H/¹³C NMR measurements. Of significant note that chain termination predominantly occurred through β -elimination (up to 84.5%), yielding vinyl-terminated long-chain olefins. These functional α -macro-olefins are valuable as precursors for postfunctionalization, expanding the potential applications of polyethylene across various sectors.



KEYWORDS: Bis(imino)pyridylcobalt precatalysts, ethylene polymerization, moderate polymer molecular weight polyethylene, linear α -macro-olefins, β -elimination reaction

INTRODUCTION

Coordination–insertion ethylene (oligo)polymerization is a versatile method to generate a wide range of products with great variations in the microstructure and chain lengths.^{1–3} These polymer products can be classified by chain length into low to high olefins, low molecular weight waxes, and high to ultrahigh molecular weight polymers, with structures ranging from strictly linear to branched and hyperbranched.^{4–7} Short-to medium chain α -olefins are used as key comonomers in low-density polyethylene and precursors for plasticizing alcohols, surfactants, lubricants, detergents, and paper sizing;^{8,9} and higher α -olefins are used to synthesize heavy linear alkyl benzene and enhance wax properties.^{10,11} Additionally, the terminal vinyl bond in long-chain α -macro-olefins enables various transformations to produce functional linear polyethylenes. Synthesizing such functional products from ethylene alone largely depends on the choice of catalyst as well as the reaction conditions. Ziegler–Natta catalysts, Phillips catalysts, metallocenes, and early transition metal catalysts are highly effective for producing high-density and strictly linear polyethylene.^{12–18} Alpha-diimine and iminopyridine nickel/palla-

dium complexes, known for their chain-walking capability, generate branched to hyperbranched polyethylene from only ethylene.¹⁹ The bis(imino)pyridine-iron/cobalt complexes, discovered in 1998, produce highly linear polyethylene with varied molecular weights (A, Figure 1).^{20–22} The recent modifications in the ligand framework of these catalysts have enabled the production of a variety of products, including short-chain to long-chain α -olefins waxes (C₄–C₂₀) and, recently, long-chain α -macro-olefins (C₂₀₊) and saturated low molecular weight waxes to high molecular weight polyethylenes.²³ In particular, 2-imino-1,10-phenathrolines-iron complex catalysts demonstrated great success in synthesis of selective ethylene oligomerization at industrial scale.²⁴

Received: August 19, 2024

Revised: September 14, 2024

Accepted: September 18, 2024

Published: September 26, 2024



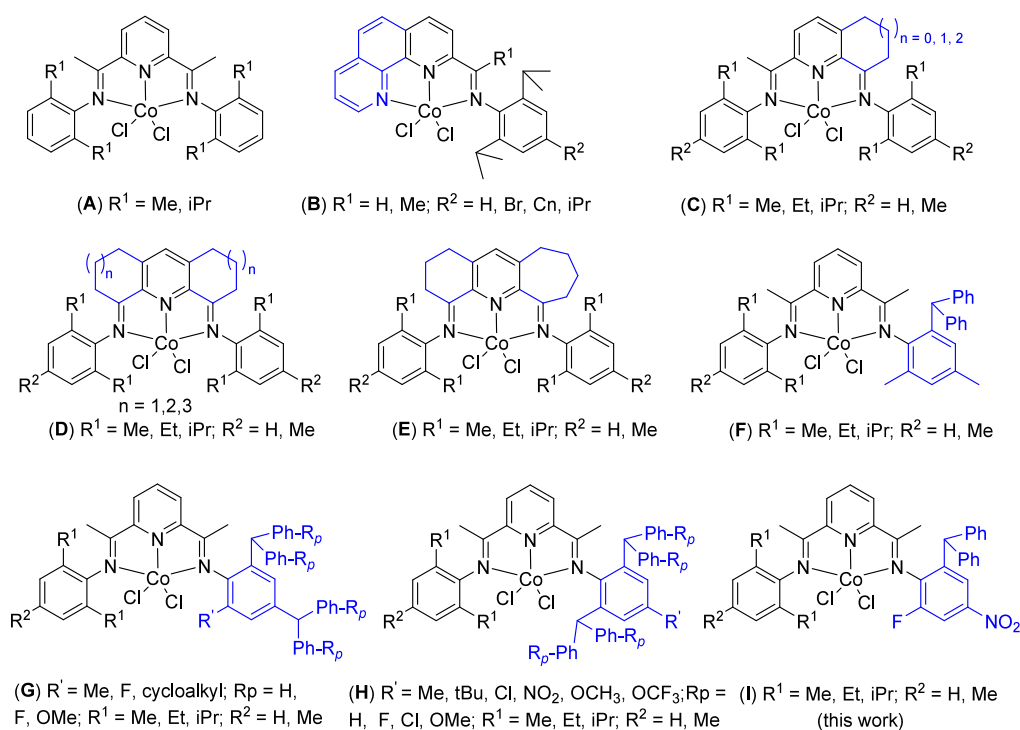


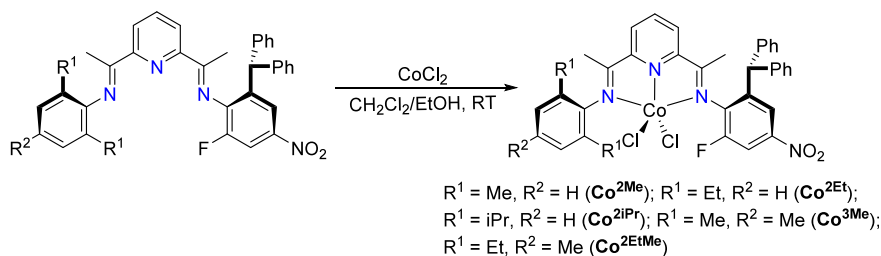
Figure 1. Selected bis(imino)pyridylcobalt precatalysts (A–H) with variations at the imine-N and central pyridine were used for ethylene polymerization, along with the precatalyst developed in this work (I).

The 2,6-bis(imino)pyridine cobalt complexes are prone to chain transfer, resulting in the production of low molecular weight polyethylene.²⁵ The molecular weight value is primarily influenced by the ligand framework and steric/electronic factors. Therefore, extensive research has focused on varying imine-N and the central pyridine unit to investigate their catalytic behavior for ethylene polymerization, and in turn produce high activities and varying microstructures.²⁶ For instance, modifying the backbone of the parent bis(imino)pyridine ligand led to the creation of imino-phenanthroline-cobalt complexes (B, Figure 1).²⁷ These precatalysts exhibited modest activity in ethylene oligomerization, primarily producing linear α -olefins with some internal olefins. Fusing a 5-, 6-, or 7-membered carbocyclic ring at 2 and 3 positions of pyridine (C, Figure 1) resulted in polyethylene with low to moderate molecular weights and a high proportion of terminal double bonds (up to 95%).^{28a–g,29} On the other hand, incorporating cyclohexyl rings on both sides of the pyridine (D, Figure 1) yielded a variety of products including low molecular weight polyethylene wax, α -olefin with Schulz Flory distribution, or 1-butene (up to 93% selectivity),²⁹ while their analogues with cycloheptyl fused ring along with sterically bulky N-aryl groups gave low to high molecular weight polyethylene with high catalytic activities and thermal stability (D, Figure 1).^{30a–e} Additionally, variants containing cycloheptyl/cyclohexyl fused rings efficiently generated low molecular weight, vinyl-terminated polyethylene with thermal stability up to 60 °C (E, Figure 1).^{30f,g} Using the parent 2,6-bis(imino)pyridine ligand with sterically bulky imine units resulted in exceptionally high activities, comparable to iron-based precatalysts in most cases, and produced polyethylene with molecular weights ranging from moderate (≈ 10 kg/mol) to high (≈ 100 kg/mol), with controlled dispersity (F–H, Figure 1).^{31–47} In particular, cobalt precatalysts with 2,6-ortho

benzhydryl steric groups and strong electron-withdrawing substituents (e.g., $R = \text{Cl, NO}_2, \text{OCF}_3$) achieved excellent activity (up to $13.7 \times 10^6 \text{ g mol}^{-1} \text{ h}^{-1}$) and produced high molecular weight polyethylene (up to 825 kg/mol) with controlled molecular weight distributions across a broad temperature range of 50–80 °C (H, Figure 1).^{38–47} These results suggest that catalysts with strong electron-withdrawing groups and larger axial substituents generally promote chain growth reactions during polymerization, leading to a high molecular weight polyethylene. Conversely, excessive steric hindrance at axial sites can hinder monomer insertion and chain growth, resulting in minimal polymer formation.^{38,40–42,44} Additionally, smaller axial steric hindrance tends to facilitate chain transfer reactions, producing low molecular weight polyethylene waxes or oligomers. Therefore, the catalytic activity, thermal stability, and molecular weight dispersity can be optimized by carefully balancing the steric and electronic factors in the ligand structure.

This study introduces a new class of bis(imino)pyridine cobalt complex catalysts by integrating *ortho*-benzhydryl as axial steric bulk, and NO_2 and F groups as strong electron-withdrawing substituents for ethylene polymerization under diverse conditions (I, Figure 1). These precatalysts with a relatively open structure displayed excellent polymerization activity and high thermal stability and produced polyethylene with moderate molecular weights. Compared with previously reported bis(imino)pyridylcobalt precatalysts, these complexes exhibited comparatively higher catalytic performance. Microstructural analysis revealed up to 84.5% terminal double bonds, which are valuable for postfunctionalization and new polymer synthesis. Moreover, as these complexes are entirely new, detailed characterization is provided.

Scheme 1. Synthesis of Cobalt Complexes



RESULTS AND DISCUSSION

Synthesis and Characterization of Cobalt Complexes

The bis(imino)pyridine ligands used in this study were prepared based on our previous reported work,⁴⁸ and their cobalt chloride complexes, 2-[MeC=N{2-(Ph₂CH)-4-NO₂-6-F}C₆H₂]-6-[MeC=N(Ar)]C₅H₃N-CoCl₂ (Ar = 2,6-Me₂C₆H₃, Co^{2Me}, 2,6-Et₂C₆H₃, Co^{2Et}, 2,6-iPr₂C₆H₃, Co^{2iPr}, 2,4,6-Me₃C₆H₂, Co^{3Me}, and 2,6-Et₂-4-MeC₆H₂, Co^{2EtMe}) were prepared by the treatment of cobalt chloride (0.95 equiv) in dichloromethane/ethanol solution, affording excellent yields (Scheme 1). The structures of all newly developed complexes were well determined using multiple characterization techniques including elemental analysis, FT-IR spectroscopy, and single-crystal X-ray diffraction study (only in the case of Co^{2Et} and Co^{2EtMe}). In the FTIR spectra, the stretching vibrations for $\nu(\text{C}=\text{N})$ imine functionality in the cobalt complexes appear around 1627 cm⁻¹, which is slightly lower than those observed in the noncoordinated ligands (Figures S13–S17). This wavenumber shift, well-documented in prior studies, highlights the successful synthesis of the cobalt complexes^{35,37} and indicates effective coordination between the imine groups and cobalt centers. Furthermore, the analysis of C, H, and N confirmed the high purity of the title complexes.

The single crystals of Co^{2Et} and Co^{2EtMe} were analyzed by X-ray diffraction, and their molecular structures are depicted in the ORTEP views shown in Figures 2 and 3, respectively. The structure refinements for both complexes are given in Table S1, and selected bond lengths and angles are summarized in Table

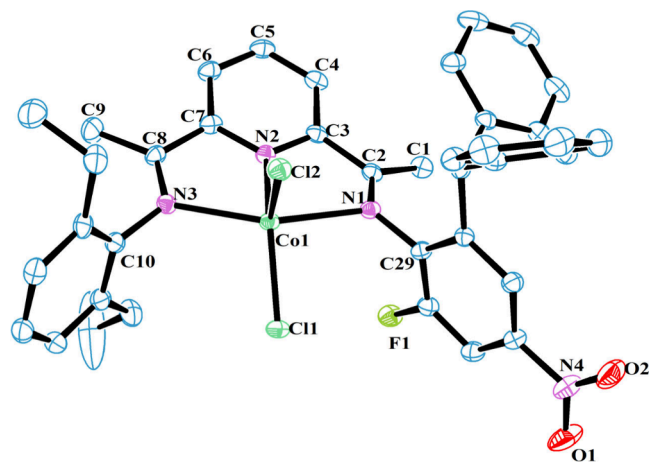


Figure 2. ORTEP views of Co^{2Et} along with thermal ellipsoids of molecular structures shown at a 30% probability level. All hydrogen atoms are removed to make a clear view, and one methyl group of the ethyl moiety, which was disordered, was also removed for a clearer view.

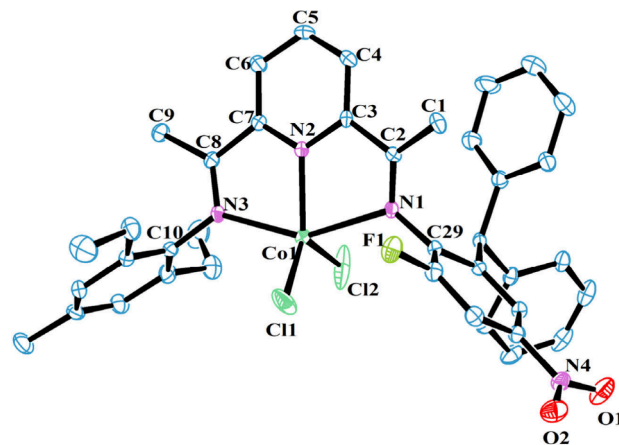


Figure 3. ORTEP views of Co^{2EtMe} along with thermal ellipsoids of molecular structures shown at a 30% probability level. All hydrogen atoms are removed to make a clear view.

1. Each complex has a penta-coordination sphere with slightly distorted square pyramidal geometry around the cobalt center. This geometry is quantitatively characterized by τ values, calculated as $\tau = 0.25$ for Co^{2Et} and $\tau = 0.45$ for Co^{2EtMe}, where τ_3 is defined as $(\beta - \alpha)/60$, with β representing the largest X-M-X angle and α the second largest angle in the coordination sphere.⁴⁹ The planes of the arylimino groups are oriented orthogonally to the plane defined by the cobalt and three nitrogen atoms. The cobalt atom is situated above the basal plane, with vertical distances of 0.629 Å for Co^{2Et} and 0.727 Å for Co^{2EtMe}. It is found that the introduction of benzhydryl substituents at the *ortho* position of one arylimino group resulted in an increase in the Co–N_{imine} bond distance by 0.089 Å for Co^{2Et} or 0.161 Å for Co^{2EtMe} compared to the arylimino group lacking the bulky substituent (Table 1). This increase is primarily due to the steric hindrance imposed by the *ortho*-benzhydryl group, which influences the bond distances. On the other hand, the Co–N_{pyridine} bond distance is significantly shorter than the Co–N_{imine} bond distance, highlighting the superior coordination ability of the pyridine nitrogen with the metal center.^{35,45,48} Moreover, within the chelate rings, the angles N1–Co1–N2 and N2–Co1–N3 are similar across both complexes; however, N2–Co1–N3 is slightly larger than N1–Co1–N2 by 2.1° for Co^{2Et} and 3.61° for Co^{2EtMe}. This variation is again attributed to the distinct steric environments around the metal center caused by the different N-aryl groups. Such features are characteristic of cobalt(II) complexes with tridentate bis(imino)pyridine ligands in a 1:1 ratio.^{21,22,50}

Table 1. Selected Bond Lengths (Å) and Angles (deg) for Co^{2Et} and Co^{2EtMe}

	Bond lengths (Å)			Angles (deg)	
	Co ^{2Et}	Co ^{2EtMe}		Co ^{2Et}	Co ^{2EtMe}
Co(1)–Cl(1)	2.2412(8)	2.2104(12)	Cl(1)–Co(1)–Cl(2)	115.18(3)	118.76(8)
Co(1)–Cl(2)	2.2661(9)	2.2376(13)	N(1)–Co(1)–N(2)	73.93(10)	73.11(10)
Co(1)–N(1)	2.290(3)	2.361(3)	N(1)–Co(1)–N(3)	149.00(9)	149.48(10)
Co(1)–N(2)	2.035(2)	2.031(3)	N(1)–Co(1)–Cl(1)	92.67(7)	90.61(8)
Co(1)–N(3)	2.201(3)	2.200(3)	N(1)–Co(1)–Cl(2)	99.54(7)	95.93(8)
N(1)–C(2)	1.284(4)	1.280(4)	N(2)–Co(1)–Cl(1)	136.90(8)	126.03(10)
N(1)–C(29)	1.418(4)	1.404(4)	N(2)–Co(1)–Cl(2)	107.46(8)	113.99(11)
N(2)–C(3)	1.334(4)	1.345(4)	N(2)–Co(1)–N(3)	76.03(10)	76.72(11)
N(2)–C(7)	1.353(4)	1.339(4)	N(3)–Co(1)–Cl(1)	104.18(7)	103.61(8)
N(3)–C(8)	1.286(4)	1.287(4)	N(3)–Co(1)–Cl(2)	96.56(7)	100.39(9)
N(3)–C(10)	1.437(4)	1.446(4)			

Ethylene Polymerization

Besides the structure of the precatalyst, reaction settings dramatically influence both catalytic behavior and the final polymer properties.^{31–47} Therefore, the effects of cocatalysts (MAO, MMAO), temperature (30–100 °C), time (5–60 min), and ethylene pressure (0.1–1 MPa) are initially examined to obtain the optimal conditions. Subsequently, the catalytic capacity of all titled cobalt complexes was studied at optimal conditions.^{35,45,48} In addition, a detailed comparison was made with previously reported bis(imino)pyridine cobalt complexes for ethylene polymerization. The units for activity and molecular weights (M_w) of PE are typically expressed as $\text{g mol}^{-1} \text{h}^{-1}$ and g mol^{-1} , respectively.

Ethylene Polymerization with Co/MAO Catalytic System

Initially, cobalt complex Co^{2Et} was used as the test precatalyst to screen the optimal conditions (Table 2, entries 1–17). In situ activation of Co^{2Et} with varying amounts of MAO (Al/Co = 1000, 1500, 2000, 2500) resulted in the highest catalytic activity of $4.91 \times 10^6 \text{ g mol}^{-1} \text{h}^{-1}$ with M_w of $38.3 \times 10^3 \text{ g mol}^{-1}$ at 1500 [conditions: temperature = 30 °C, time = 30 min, ethylene = 1 MPa]. As shown in Figure 4a, the data exhibited a bell-shaped curve: activity increased with the cocatalyst concentration, peaked at 1500, and then gradually declined (entries 1–4). In contrast, polymer molecular weight (M_w) continuously decreased from 57.8×10^3 to $26.0 \times 10^3 \text{ g mol}^{-1}$ as cocatalyst concentration rose. Low cocatalyst concentrations are insufficient, while excessive amounts may reduce activity, likely due to catalyst deactivation or inhibition. Additionally, higher concentrations of the aluminum compound in the reaction mixture may favor chain termination over chain propagation, leading to reduced polymer molecular weights.^{35,45} This behavior is typical of bis(imino)pyridine cobalt precatalysts. As can see in the Figure 5a, the M_w dispersity remained broad and unimodal across all concentration of cocatalyst and became even broader at higher concentrations ($M_w/M_n = 12.5–15.4$), which is also an indication of higher chain transfer reactions occurrence at higher concentration of cocatalyst.⁵¹

The polymerization results in Table 2 (entries 2 and 5–11) demonstrated that both catalytic activity and polymer molecular weights were significantly influenced by reaction temperature [Al/Co = 1500, time = 30 min, ethylene = 1 MPa]. The relationship between catalytic activity and temperature (30–100 °C) also followed a bell-shaped curve: activity initially increased, reached a maximum of $9.66 \times 10^6 \text{ g mol}^{-1} \text{h}^{-1}$ at 60 °C, and then gradually dropped to a minimum of

$0.45 \times 10^6 \text{ g mol}^{-1} \text{h}^{-1}$ at 100 °C (Figure 4b). On the other hand, polymer M_w gradually decreased from $57.8 \times 10^3 \text{ g mol}^{-1}$ to $18.9 \times 10^3 \text{ g mol}^{-1}$ with reaction temperature (entries 2, 5–11, Figure 4b). The decline in activity at higher temperatures was in principal due to the decomposition of active species, while gradient decrease of ethylene concentration in the reaction mixture may also contribute to lower the catalytic activity.⁵² Generally, it is accepted that elevated temperatures promote chain transfer reactions relative to the chain growth reactions (k_{tr}/k_{ins}), which resulted in lower molecular weight polyethylene. The molecular weight distribution was broad and unimodal with a small high-molecular-weight tail across all temperatures (Figure 5b), and the gradual broadening of the M_w dispersity further supported the occurrence of increased chain transfer reactions at higher temperatures ($M_w/M_n = 14.0–16.2$).

The polymerization results in Table 2 (entries 7, 12–15) summarized the effect of reaction time [conditions: Al/Co = 1500, temperature = 60 °C, and ethylene = 1 MPa]. These results showed the high stability of the Co^{2Et}/MAO catalyst system at 60 °C. Both polymer yield and molecular weights increased with longer reaction times, achieving the highest activity of $27.6 \times 10^6 \text{ g mol}^{-1} \text{h}^{-1}$ at 5 min (entries 7, 12–15). However, activity gradually dropped with extended reaction times (Figure 4c), likely due to polymer mass removal and the gradual decomposition of the active catalytic species.^{19,53} Despite this drop, the system sustained a significant activity of $5.8 \times 10^6 \text{ g mol}^{-1} \text{h}^{-1}$ even after 60 min at 60 °C (entry 15). The molecular weight of the polyethylene improved from 13.0×10^3 to $23.2 \times 10^3 \text{ g mol}^{-1}$ with longer reaction times (Figure 4c), due to the continuous dominance of chain growth over chain transfer reactions. Additionally, the molecular weight dispersity decreased with time ($M_w/M_n = 9.42–14.4$), indicating reduced chain transfer reactions at longer times (Figure 5c). Overall, these results highlight the robust stability of the Co^{2Et}/MAO catalyst system, maintaining high activity and polymer molecular weight over a 60 min period at 60 °C.

To evaluate the effect of pressure on ethylene polymerization, three reactions in a row were carried out with different ethylene pressures in the range of 0.1–1 MPa [conditions: Al/Co = 1500, temperature = 60 °C, time = 30 min]. Increasing the ethylene pressure from 0.1 to 0.5 MPa led to a 150% increase in activity (entries 16, 17). Further raising the pressure to 1.0 MPa resulted in an additional 140% increase in activity (entries 7, 17). These results indicate a significant dependence of polymerization activity on ethylene pressure, with the increased activity attributed to the higher ethylene

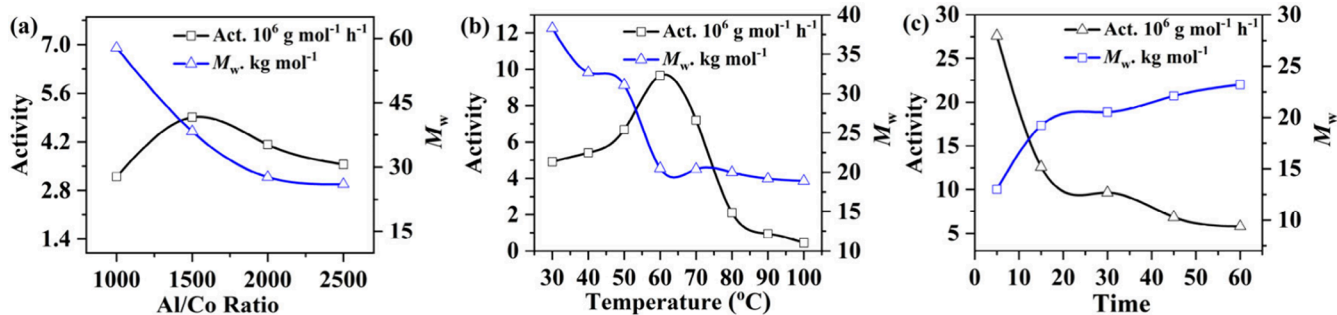


Figure 4. Polymerization activity and polymer molecular weights, using $\text{Co}^{2\text{Et}}/\text{MAO}$ at different Al/Co ratios (a), temperatures (b), and times (c) at 1 MPa ethylene pressure.

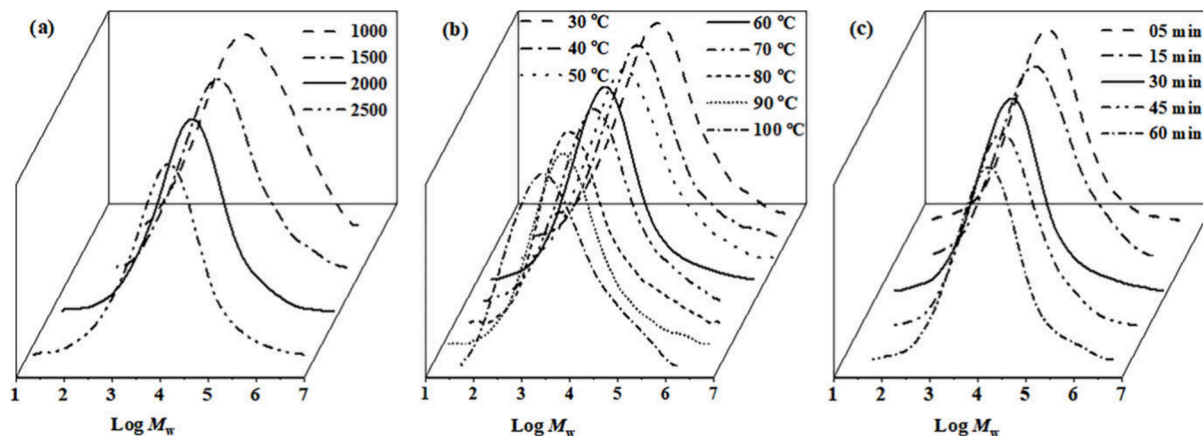


Figure 5. GPC curves at different cocatalyst amounts (a), temperatures (b), and times (c) using $\text{Co}^{2\text{Et}}/\text{MAO}$ as the catalytic system at 1 MPa ethylene pressure.

concentration in toluene at elevated pressures.^{19,54} Additionally, the molecular weight of the resulting polyethylene showed a linear relationship with ethylene pressure, increasing from 17.6×10^3 to $20.5 \times 10^3 \text{ g mol}^{-1}$, accompanied by a unimodal and broad dispersity ($M_w/M_n = 8.60\text{--}14.4$).^{48–51}

With the aim to investigate steric and electronic substituents of aniline (Scheme 1), the catalytic performance of other prepared cobalt precatalysts ($\text{Co}^{2\text{Me}}$, $\text{Co}^{2\text{iPr}}$, $\text{Co}^{3\text{Me}}$, and $\text{Co}^{2\text{EtMe}}$) was examined using the optimal conditions determined for $\text{Co}^{2\text{Et}}/\text{MAO}$ (Table 2, entries 7, 18–21). The observed activities for all precatalysts are generally high, falling in the range of $7.20\text{--}13.3 \times 10^6 \text{ g mol}^{-1} \text{ h}^{-1}$ and are greatly influenced by the steric properties of the *ortho* substituents and electronic substituent of *para* substituents present on the small N-aryl group (Figure 6a).^{35,45} For comparison purposes, prepared cobalt complexes are classified

into two groups: group A [$\text{Co}^{2\text{Me}}$, $\text{Co}^{2\text{Et}}$, $\text{Co}^{2\text{iPr}}$] bearing different *ortho* substituents and *para*-hydrogen; group B [$\text{Co}^{3\text{Me}}$, $\text{Co}^{2\text{EtMe}}$] bearing different *ortho* and *para*-methyl substituents. It is found that the second group of cobalt complexes bearing *para*-methyl substituents exhibited comparatively lower activities than their counterpart bearing *para*-hydrogen substituent. For instance, $\text{Co}^{2\text{Me}}$ exhibited an activity of $13.3 \times 10^6 \text{ g mol}^{-1} \text{ h}^{-1}$, which is slightly higher than that of activity obtained with $\text{Co}^{3\text{Me}}$ (entry 18 vs 20) and a similar result was found on comparison with $\text{Co}^{2\text{Et}}$ with $\text{Co}^{2\text{EtMe}}$ (entry 7 vs 21). This fact highlights the negative effect of the electron donating *para*-methyl substituent on activity; perhaps the electron releasing effect decreases the Lewis acidic character of the metal center which in turn somehow reduces the rate of monomer coordination–insertion. Within the cobalt complexes of group A, the catalytic activity shows an inverse relationship with the increasing steric hindrance of the *ortho*-R substituents. For instance, $\text{Co}^{2\text{Me}}$ displayed higher activity than that of $\text{Co}^{2\text{Et}}$ by a factor of 1.4 and higher than that of $\text{Co}^{2\text{iPr}}$ by a factor of 1.9 (entries 7 vs 18 and 19). The complex $\text{Co}^{2\text{iPr}}$ was found to be the least active precatalyst due to bearing a sterically bulky *ortho* substituent (entry 19). This is likely the result of the less hindered *ortho*-R substituent allowing for easier ethylene coordination and insertion at the active sites. Overall, based on the steric and electronic substituent on the aniline, activities decreased as follows: $\text{Co}^{2\text{Me}}$ ($R^1 = \text{Me}$, $R^2 = \text{H}$) > $\text{Co}^{3\text{Me}}$ ($R^1 = \text{Me}$, $R^2 = \text{Me}$) > $\text{Co}^{2\text{Et}}$ ($R^1 = \text{Et}$, $R^2 = \text{H}$) > $\text{Co}^{2\text{EtMe}}$ ($R^1 = \text{Et}$, $R^2 = \text{Me}$) > $\text{Co}^{2\text{iPr}}$ ($R^1 = \text{iPr}$, $R^2 = \text{H}$).

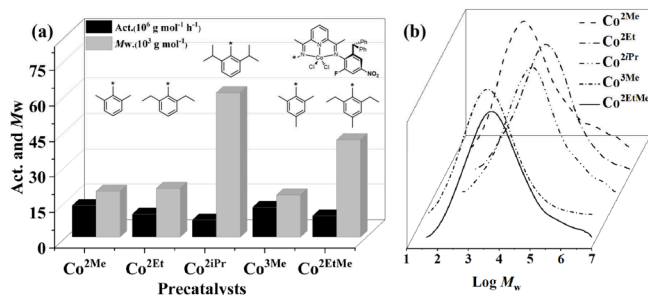


Figure 6. Comparison of polymerization activity and M_w (a) and GPC curves (b) for different precatalysts using MAO (Table 2).

Table 2. Ethylene Polymerization with Co/MAO Catalytic System^a

Entry	Precat.	Al/Co	T (°C)	t (min)	PE (g)	Act. ^b	M _w ^c	M _w /M _n ^c	T _m (°C) ^d	X _c (%) ^d
1	Co ^{2Et}	1000	30	30	3.20	3.20	57.8	12.5	135.2	42.7
2	Co ^{2Et}	1500	30	30	4.91	4.91	38.3	12.9	132.0	43.4
3	Co ^{2Et}	2000	30	30	4.12	4.12	27.7	14.2	130.5	42.9
4	Co ^{2Et}	2500	30	30	3.55	3.55	26.0	15.4	129.5	41.7
5	Co ^{2Et}	1500	40	30	5.40	5.40	32.7	14.0	129.7	42.1
6	Co ^{2Et}	1500	50	30	6.67	6.67	31.1	14.0	130.3	41.5
7	Co ^{2Et}	1500	60	30	9.66	9.66	20.5	14.4	127.8	37.4
8	Co ^{2Et}	1500	70	30	7.20	7.20	20.4	14.7	130.2	38.5
9	Co ^{2Et}	1500	80	30	2.10	2.10	20.0	15.4	130.3	39.5
10	Co ^{2Et}	1500	90	30	0.94	0.94	19.2	15.9	128.4	26.8
11	Co ^{2Et}	1500	100	30	0.45	0.45	18.9	16.2	132.4	35.2
12	Co ^{2Et}	1500	60	05	4.42	27.6	13.0	11.6	127.8	36.9
13	Co ^{2Et}	1500	60	15	6.31	12.6	19.2	10.3	129.7	37.6
14	Co ^{2Et}	1500	60	45	10.3	6.86	22.1	9.70	128.9	39.4
15	Co ^{2Et}	1500	60	60	11.6	5.80	23.2	9.42	129.2	38.0
16 ^e	Co ^{2Et}	1500	60	30	1.67	1.67	17.6	8.60	130.0	38.4
17 ^f	Co ^{2Et}	1500	60	30	4.13	4.13	19.3	8.60	131.7	42.8
18	Co ^{2Me}	1500	60	30	13.3	13.3	19.3	9.3	127.3	33.8
19	Co ^{2iPr}	1500	60	30	7.20	7.20	61.0	8.0	131.5	49.4
20	Co ^{3Me}	1500	60	30	12.5	12.5	17.7	9.1	125.9	31.0
21	Co ^{2EtMe}	1500	60	30	8.93	8.93	41.1	9.5	130.0	44.5

^aConditions: precat. (2.0 μmol), solvent (toluene, 100 mL), ethylene (1 MPa). ^bActivity: 10⁶ g mol⁻¹ h⁻¹. ^cGPC results (M_w, 10³ g mol⁻¹). ^dDetermined by DSC, X_c = 100 × ΔH_f(T_m)/ΔH_f^o(T_m), where ΔH_f^o(T_m) = 248.3 J g⁻¹. ^eEthylene (0.1 MPa). ^fEthylene (0.5 MPa).

Table 3. Ethylene Polymerization with Co/MMAO Catalytic System^a

Entry	Precat.	Al/Co	T (°C)	t (min)	PE (g)	Act. ^b	M _w ^c	M _w /M _n ^c	T _m (°C) ^d	X _c (%) ^d
1	Co ^{2Et}	1000	30	30	2.80	2.80	14.4	6.5	129.0	42.2
2	Co ^{2Et}	1500	30	30	3.61	3.61	13.8	7.5	128.6	40.3
3	Co ^{2Et}	2000	30	30	3.99	3.99	9.15	7.6	128.0	36.9
4	Co ^{2Et}	2500	30	30	3.67	3.67	8.63	9.5	128.4	37.3
5	Co ^{2Et}	2000	40	30	5.40	5.40	8.00	8.4	126.6	37.5
6	Co ^{2Et}	2000	50	30	4.93	4.93	7.83	8.5	126.3	33.5
7	Co ^{2Et}	2000	60	30	4.74	4.74	7.61	8.6	126.5	38.3
8	Co ^{2Et}	2000	70	30	3.70	3.70	7.55	8.7	126.6	32.9
9	Co ^{2Et}	2000	80	30	3.42	3.42	7.40	8.8	126.2	30.9
10	Co ^{2Et}	2000	90	30	0.96	0.96	7.35	9.0	126.4	33.1
11	Co ^{2Et}	2000	100	30	0.51	0.51	7.33	9.6	129.3	24.0
12	Co ^{2Me}	2000	40	30	4.32	4.32	7.0	10.0	124.4	17.2
13	Co ^{2iPr}	2000	40	30	3.68	3.68	31.6	7.0	130.9	45.7
14	Co ^{3Me}	2000	40	30	4.54	4.54	8.5	9.9	125.7	24.3
15	Co ^{2EtMe}	2000	40	30	5.20	5.20	27.2	11.4	130.4	37.4

^aConditions: precat. (Co^{2Et}, 2.0 μmol), solvent (toluene, 100 mL), ethylene (1 MPa). ^bActivity: 10⁶ g mol⁻¹ h⁻¹. ^cGPC results (M_w, 10³ g mol⁻¹). ^dDetermined by DSC, X_c = 100 × ΔH_f(T_m)/ΔH_f^o(T_m), where ΔH_f^o(T_m) = 248.3 J g⁻¹.

Prior studies have reported that steric hindrance over the axial sites of the metal center favors chain growth reactions over the chain transfer reactions, thus producing high molecular weight polyethylene.^{40,45,47} Consistent with these reports, cobalt complexes bearing sterically bulky *ortho*-alkyl substituents produced comparatively higher molecular weight polyethylene (Figure 6a). Within group A, steric hindrance decreased in the order Co^{2iPr} > Co^{2Et} > Co^{2Me} and polymer M_ws also decreased in the same order. For instance, replacement of the *ortho*-methyl group in Co^{2Me} by the *ortho*-ethyl group in Co^{2Et} gave a slight improvement in the M_w from 19.3 × 10³ to 20.3 × 10³ g mol⁻¹ and replacement by isopropyl group in Co^{2iPr} gave about 220% increase in the polymer molecular weight, highlighting how steric hindrance protects the active species from chain transfer reactions.

Moreover, Co^{2EtMe} containing a *para*-methyl group generated polyethylene with a higher molecular weight than that of polyethylene obtained with Co^{2Et} bearing *para*-hydrogen. The impact of the *para*-methyl substituent on molecular weights remains uncertain, perhaps due to electron releasing effect of *para*-methyl group increasing the chain growth reactions over the chain transfer reactions, thus generating higher molecular weight polyethylene. The molecular weight distributions were unimodal and broad in all cases, and likely more than one type of active species was involved in chain propagation (Figure 6b). The broad dispersity is likely the result of high chain transfer reactions as the molecular weight range was moderately varied from 17.7 to 61.0 × 10³ g mol⁻¹.^{44,46} Moreover, high melt temperature is characteristic of all obtained polyethylene from all cobalt precatalysts which varied

in the range of 125.9–131.5 °C with high crystallinity ($X_c = 33.8$ –49.4%).

Ethylene Polymerization with Co/MMAO Catalytic System

To thoroughly compare and assess the effect of cocatalysts on catalytic activity, another cocatalyst, MMAO, was used to re-evaluate the catalytic capacity of cobalt complexes for ethylene polymerization under the same conditions. As was the case of MAO, $\text{Co}^{2\text{Et}}$ in activation with MMAO was selected as the test catalytic system to optimize the reaction conditions. Table 3 shows the results for different Al/Co ratios (1000, 1500, 2000, and 2500). The dependence of catalytic activity and polymer molecular weights upon changing the cocatalyst amount followed a similar relationship as was observed in the case of MAO (Figure S1a). The highest activity of $3.99 \times 10^6 \text{ g mol}^{-1} \text{ h}^{-1}$ was achieved with an Al/Co ratio of 2000 (entry 3), while lower or higher ratios resulted in lower activities (entries 1–2, 4). The highest polymer molecular weight of $14.4 \times 10^3 \text{ g mol}^{-1}$ was achieved at Al/Co ratio of 1000 and further increase of cocatalyst concentration resulted in gradual decrease, reached to the lowest value of $8.63 \times 10^3 \text{ g mol}^{-1}$ at Al/Co ratio of 2500. This suggests that higher cocatalyst concentration promotes chain transfer reactions over chain propagation.^{35–45} The increase of dispersity values with cocatalyst amount further supports the higher chain transfer reactions at higher cocatalyst concentrations ($M_w/M_n = 6.5$ –9.5) (Figure S2a). Compared with the $\text{Co}^{2\text{Et}}$ /MAO system, the $\text{Co}^{2\text{Et}}$ /MMAO system produced polyethylene with narrower molecular weight distributions. However, the $\text{Co}^{2\text{Et}}$ /MMAO system was less efficient, showing about 20% lower activity and 75% lower polymer molecular weight compared to the $\text{Co}^{2\text{Et}}$ /MAO system (Table 2, entries 1 and 2 vs Table 3, entries 1 and 3).^{55,56}

Changes in the reaction temperature between 30 and 100 °C revealed that the highest activity of $5.40 \times 10^6 \text{ g mol}^{-1} \text{ h}^{-1}$ occurred at 40 °C (Table 3, entries 3, 5–11). Activity decreased as the temperature elevated beyond this point (Figure S1b). The decrease in activity was relatively less, only 36%, for temperatures ranging from 30 to 80 °C. However, a dramatic decline in activity occurred with a 10 °C increase from 80 to 90 °C and then to 100 °C, resulting in significant decrease in activity of 72% and 50%, respectively. This fact highlights high stability of the active species within the temperature range of 30 to 80 °C (entries 3, 5–9). Additionally, despite the molecular weight of polyethylene gradually decreasing from 9.15×10^3 to $7.33 \times 10^3 \text{ g mol}^{-1}$ with temperature, the decrease was relatively less, with only a 20% decline observed when the temperature was increased from 30 to 100 °C. This indicates a high stability of the active species and continued chain growth reactions. The slight reduction in molecular weight with rising temperature is likely due to the increase of chain transfer reactions.⁵⁷ This observation is supported by the consistent broadening of the dispersity index with the temperature (Figure S2b). Furthermore, the decreased rate of monomer insertion could be attributed to partial decomposition of the active species or/and reduced solubility of the monomer at higher temperatures.^{52,58} In comparison to MMAO, $\text{Co}^{2\text{Et}}$ demonstrated superior thermal stability when activated with MAO: the highest activity of $9.66 \times 10^6 \text{ g mol}^{-1} \text{ h}^{-1}$ was obtained at 60 °C with MAO, while 40 °C was the optimal temperature with MMAO giving an activity of $5.40 \times 10^6 \text{ g mol}^{-1} \text{ h}^{-1}$. Additionally, the molecular weight of the resulting poly-

ethylene was significantly higher with MAO than with MMAO across all studied reaction temperatures, indicating that $\text{Co}^{2\text{Et}}$ performs better in combination with MAO under various reaction conditions (Table 2, entries 2, 5–11 vs Table 3, entries 3, 5–11).

Under otherwise identical conditions (Al/Co = 2000, temperature 40 °C, ethylene = 1 MPa, time = 30 min), all tested cobalt complexes exhibited high polymerization rates, in the range of 3.68×10^6 – $5.40 \times 10^6 \text{ g mol}^{-1} \text{ h}^{-1}$ (Table 3, entries 5, 12–15). Among the complexes in group A ($\text{Co}^{2\text{Me}}$, $\text{Co}^{2\text{Et}}$, $\text{Co}^{2\text{iPr}}$) the complex $\text{Co}^{2\text{Et}}$, which contains an *ortho*-ethyl group, showed the highest activity of $5.40 \times 10^6 \text{ g mol}^{-1} \text{ h}^{-1}$ (Figure 7a).³⁸ In contrast, complexes with less steric hindrance [$\text{Co}^{2\text{Me}}$ ($R^1 = \text{Me}$, $R^2 = \text{H}$)] or more steric hindrance [$\text{Co}^{2\text{iPr}}$ ($R^1 = \text{iPr}$, $R^2 = \text{H}$)] demonstrated lower activity (entries 5, 12–13). Particularly, complex $\text{Co}^{2\text{iPr}}$, with the most *ortho* steric congestion, had the lowest polymerization activity at $3.68 \times 10^6 \text{ g mol}^{-1} \text{ h}^{-1}$ (entries 13). Meanwhile, the incorporation of *para*-methyl substituent into the small N-aryl unit had a positive impact on the rate of monomer insertion; therefore, $\text{Co}^{3\text{Me}}$ displayed slightly higher activity than that of $\text{Co}^{2\text{Me}}$. However, this trend reversed when comparing $\text{Co}^{2\text{EtMe}}$ with $\text{Co}^{2\text{Et}}$. Overall, structure–activity relationship follows an order of $\text{Co}^{2\text{Et}}$ ($R^1 = \text{Et}$, $R^2 = \text{H}$) > $\text{Co}^{2\text{EtMe}}$ ($R^1 = \text{Et}$, $R^2 = \text{Me}$) > $\text{Co}^{3\text{Me}}$ ($R^1 = \text{Me}$, $R^2 = \text{Me}$) > $\text{Co}^{2\text{Me}}$ ($R^1 = \text{Me}$, $R^2 = \text{H}$) > $\text{Co}^{2\text{iPr}}$ ($R^1 = \text{iPr}$, $R^2 = \text{H}$). This activity–structure relationship is different from one observed in the case of MAO. Moreover, cobalt complexes with sterically bulky *ortho*-substituents were more effective in producing higher molecular weight polyethylene compared to their sterically less hindered analogues (Figure 7a). For example, ethylene polymerization mediated by $\text{Co}^{2\text{iPr}}$ yielded polyethylene with a molecular weight 350% higher than that produced by $\text{Co}^{2\text{Me}}$ and about 300% higher than that of $\text{Co}^{2\text{Et}}$ (entries 1–3). A similar trend was observed when comparing the molecular weight of polyethylene from $\text{Co}^{3\text{Me}}$ to that from $\text{Co}^{2\text{EtMe}}$ ($M_w = 8.5 \times 10^3$ vs $27.2 \times 10^3 \text{ g mol}^{-1}$, respectively). Additionally, the incorporation of *para*-methyl groups in cobalt complexes proved superior compared to counterparts bearing *para*-hydrogen substituents (entries 1 and 2 vs 4 and 5). For instance, replacing $\text{Co}^{2\text{Et}}$ with $\text{Co}^{2\text{EtMe}}$ resulted in a 240% increase in the molecular weight of the obtained polyethylene. This enhancement is likely due to the electron-releasing effect of the *para*-methyl substituent, which increases the stability of the active species and facilitates chain growth reactions.^{36,38} The dispersity of the prepared PE was unimodal and broad; it is possible more than one type of active species was involved (Figure 7b). High melt temperatures ($T_m = 124.4$ °C–130.9 °C) and the high percentage of crystallinity indicate a highly linear microstructure of the polyethylene.

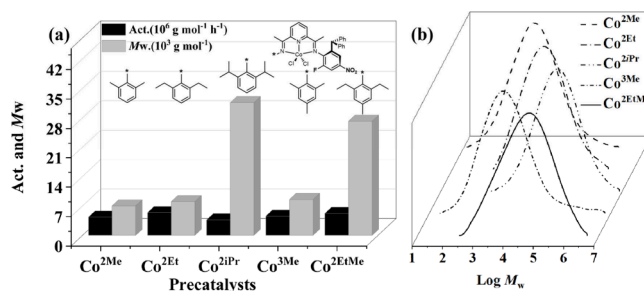


Figure 7. Comparison of polymerization activity and M_w (a) and GPC curves (b) for different precatalysts using MMAO (Table 3).

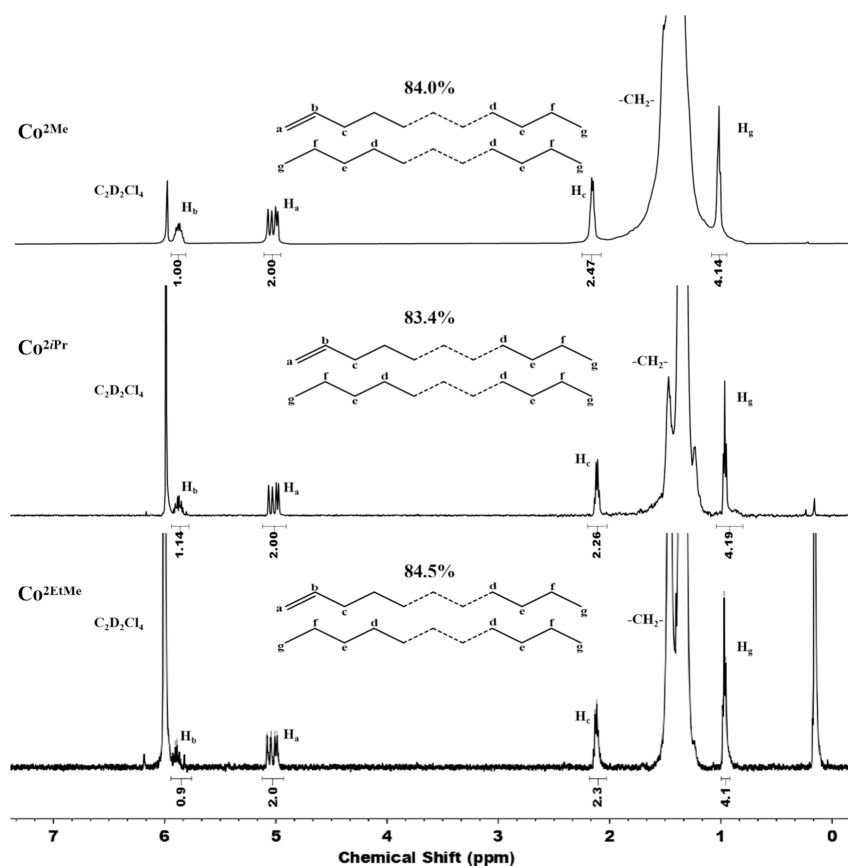


Figure 8. ^1H NMR spectrum of the polyethylene produced using $\text{Co}^{2\text{Me}}$, $\text{Co}^{2\text{iPr}}$, and $\text{Co}^{2\text{EtMe}}$ /MAO (Table 2, entries 18, 19, and 21).

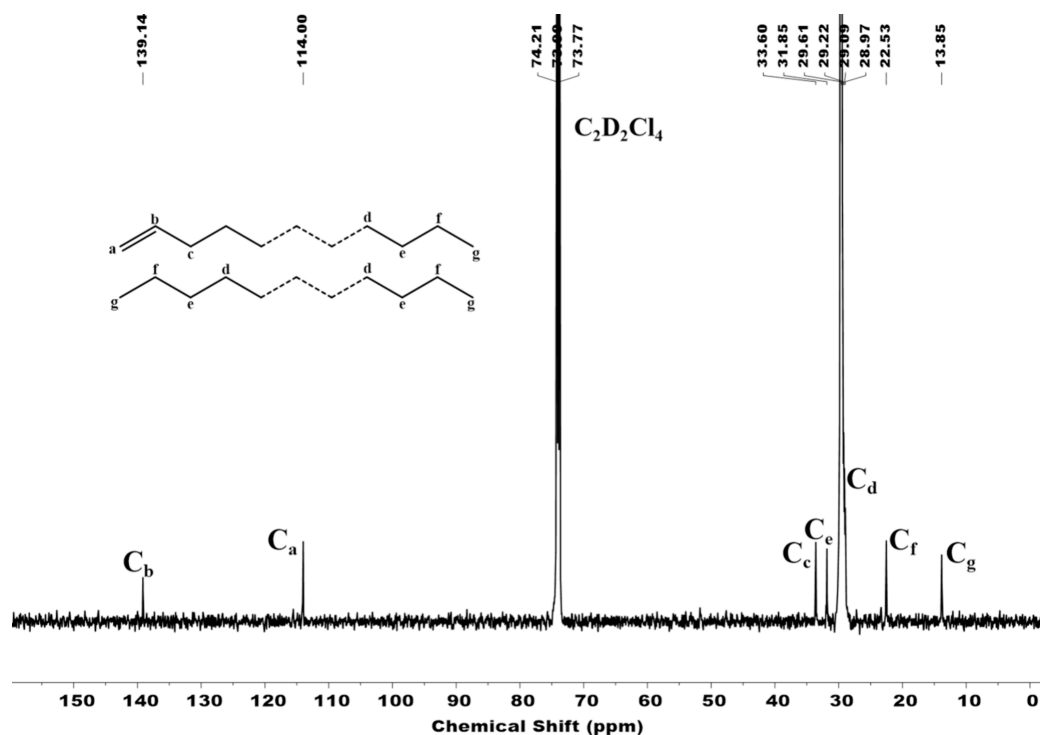


Figure 9. ^{13}C NMR spectrum of the polyethylene produced using $\text{Co}^{2\text{Me}}$ /MAO (Table 2, entry 18).

The comparison of cocatalysts revealed that MAO was identified as a more effective activator compared to MMAO for the activation of the title cobalt complexes for ethylene polymerization. In particular, $\text{Co}^{2\text{Et}}$ was the most active

precatalyst with MMAO; its activity increased by about 150% when activated with MAO. Similarly, $\text{Co}^{2\text{Me}}$ showed the highest activity with MAO, displaying about 200% higher activity compared to MMAO. In general, title complexes

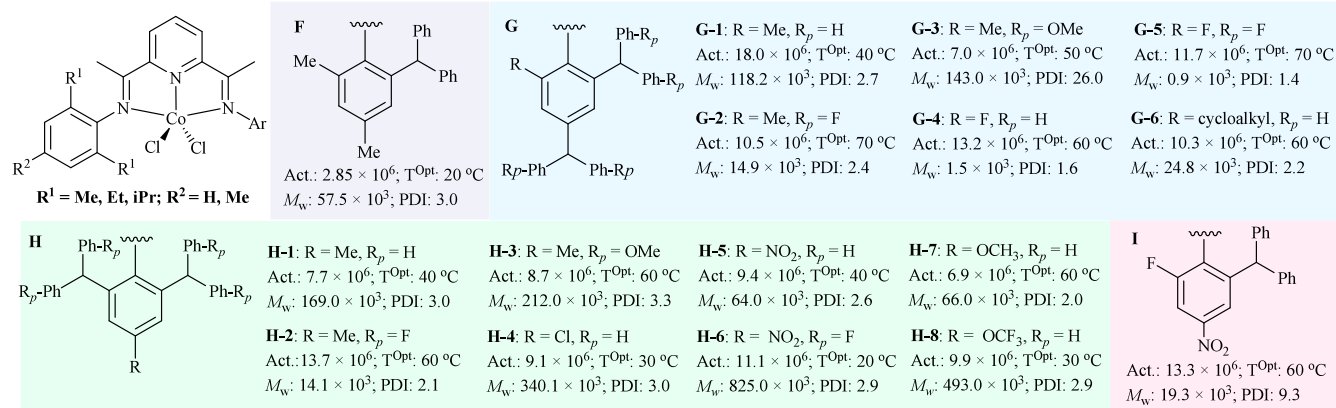


Figure 10. Comparative analysis with previously reported bis(imino)pyridylcobalt precatalysts (cocatalyst MAO or MMAO).

produced polyethylene with significantly higher molecular weight when activated with MAO rather than MMAO. Notably, MAO-activated $\text{Co}^{2\text{IPr}}$ generated polyethylene with a molecular weight about 100% higher than the same precatalyst activated with MMAO. The reasons for these differences in catalytic behavior are not fully understood but are likely due to variations in activation ability, cocatalyst composition, size, activation process, and control over chain transfer reactions.

Thermal and Microstructural Analysis of PE

The differential scanning calorimetry (DSC) analysis of polyethylene showed a sharp peak of endotherm at above 124 °C (Figures S5–S12). This implies a crystalline type of polyethylene. The crystallinity (X_c) of polyethylene was determined by using the formula $X_c = 100 \times \Delta H_f / \Delta H_f^\circ$ (T_m°), where ΔH_f° (T_m°) = 248.3 J g⁻¹ which falls in the range of 31–49% for Co/MAO and 17–46% for Co/MMAO, depending on the structure of precatalyst. High crystallinity and high melt temperatures imply the highly linear microstructure of obtained polyethylene. Further information about the structure and chain end groups were confirmed by performing ¹H/¹³C NMR measurements of selected PE samples (Table 2, entries 18, 19, 21).^{57–59} As can see in Figure 8, the ¹H NMR spectra of $\text{Co}^{2\text{Me}}$ /MAO based PE exhibited a strong singlet at the upfield region at 1.37 and 29.09 ppm in the ¹³C NMR spectrum, corresponding to the $-\text{CH}_2-$ repeating unit of the PE chain (Figure 9). Besides, two more multiplets appeared at lowfield regions around 5.05 and 5.90 ppm in the ¹H NMR spectrum, corresponding to the vinyl bond at the chain end group. These signals appeared at 139.14 and 114.0 ppm in the ¹³C NMR spectrum. Both the ¹H and ¹³C NMR spectra confirmed the strictly linear microstructure of the resulting polyethylene with vinyl $[\text{CH}_2=\text{CH}-(\text{CH}_2)_n-\text{CH}_3]$ or/and methyl chain end groups $[\text{CH}_3-(\text{CH}_2)_n-\text{CH}_3]$. Using the previously established method,^{48,60,61} the relative proportion of vinyl terminated and fully saturated polyethylene was determined and was investigated the impact of ligand structure on this proportion. Based on the H_g/H_a integration ratio, approximately 84.0% of the polyethylene chains were terminated by β -H elimination reaction, yielding vinyl end terminated PE with a strictly linear structure. The $\text{Co}^{2\text{EtMe}}$ /MAO based PE gave almost similar percentage of vinyl end terminated PE up to 84.5%, however, $\text{Co}^{2\text{IPr}}$ /MAO bearing *ortho*-isopropyl substituents produced polyethylene with 83.4% vinyl terminated polyethylene chains (Figures S3–S4). This

can be attributed to higher steric hindrance over the axial sites of the metal center protecting the active species in a better way from the β -H elimination reaction; thus, a slightly lower proportion of $\text{CH}_2=\text{CH}-(\text{CH}_2)_n-\text{CH}_3$ chains was produced in the case of $\text{Co}^{2\text{IPr}}$ /MAO mediated ethylene polymerization.

Comparative Analysis with Previously Reported Bis(imino)pyridylcobalt Precatalysts

Brookhart and Gibson were the first to explore bis(imino)pyridylcobalt precatalysts for ethylene polymerization in the late 1990s.^{14,21,22} Although their work laid the groundwork, challenges persisted, including poor catalytic activity, sub-optimal polymer molecular weight under industrial conditions, broad molecular weight distributions, low thermal stability, high cocatalyst demands, and uncontrolled chain ends. To address these issues, continuous efforts have been made to improve their catalytic performance and synthesis of new polyethylene products.^{20b} Herein, a comparison is made to evaluate the catalytic performance of the current cobalt precatalysts against previously reported bis(imino)pyridylcobalt precatalysts (Figure 10). This comparison focused on key catalytic parameters including activity, molecular weight, and dispersity at the temperature at which maximum activity was achieved in the work (called optimal temperature: T^{Opt}). For instance, precatalyst F (Figure 10) showed its peak activity of 2.85×10^6 g mol⁻¹ h⁻¹ at 20 °C and remained stable up to 60 °C.³¹ In the set of G type precatalysts, activity varied from 7.0×10^6 to 18.0×10^6 g mol⁻¹ h⁻¹, with the highest activity achieved when R = Me and $R_p = \text{H}$ (G-1, Figure 10),³² while the precatalyst with R = Me and $R_p = \text{OMe}$ produced polyethylene with the highest molecular weight ($M_w = 143.0 \times 10^3$ g mol⁻¹) but had a broad dispersity index (G-3, Figure 10).³⁴ Additionally, precatalysts with R = F and $R_p = \text{F}$ showed high thermal stability (up to 90 °C) and excellent catalytic activity of 2.7×10^6 g mol⁻¹ h⁻¹ (G-5, Figure 10).³⁶ The H type cobalt precatalysts demonstrated both excellent activity (as high as 13.7×10^6 g mol⁻¹ h⁻¹) and the ability to produce high molecular weight polyethylene (up to 825×10^3 g mol⁻¹) with controlled molecular weight distributions over a broad temperature range (50–80 °C).⁴⁵ Precatalysts with strong electron-withdrawing groups (such as R = Cl, NO₂, OCF₃) typically yielded higher molecular weight polyethylene and more controlled dispersity (H-4, -6, -8, Figure 10).^{40,45,47} With a few exceptions (G-1, H-2, Figure 10),^{32,39} the cobalt complexes reported in this study (I, Figure 10) exhibited higher catalytic activity (as high as

$13.3 \times 10^6 \text{ g mol}^{-1} \text{ h}^{-1}$), compared to all previously reported bis(imino)pyridylcobalt precatalysts. These complexes also remain effective at high reaction temperatures up to 100°C . Additionally, they produce polyethylene with moderate molecular weights over a wide temperature range ($30\text{--}100^\circ\text{C}$) without significant loss of molecular weight. Unlike previous precatalysts,^{31–47} these exhibit unimodal distributions with broad dispersity. Most notably, the polyethylene produced is vinyl-terminated (up to 84.5%), making it suitable for use as macromonomers or additives or for postfunctionalization. These exceptional characteristics are attributed to the incorporation of strong electron-withdrawing groups (*ortho*-F and *para*-NO₂) along with the sterically demanding *ortho*-benzhydryl group into the title cobalt complexes.

■ EXPERIMENTAL SECTION

Synthesis of Ligands

The synthesis of bis(imino)pyridine ligands used in this study were prepared and characterized based on our previous reported work.⁴⁸

Synthesis of Complexes

Synthesis of Co^{2Me} (General Procedure). Under an inert atmosphere, a Schlenk tube was filled with ligand L^{2Me} (0.150 g, 0.26 mmol) and CoCl₂ (0.032 g, 0.25 mmol), followed by the addition of 10 mL of dist. ethanol and 5 mL of dist. dichloromethane, it was then stirred for 12 h. Next, the solvent was totally removed under vacuum. The product was recrystallized with the addition of 10 mL of diethyl ether and then washed three times. After filtration, the resulting solid was vacuum-dried, yielding the light green Co^{2Me} complex (0.140 g, Yield: 76%). FTIR (KBr, cm⁻¹): 3088 (w), 3027 (w), 2914 (m), 1645 (w), 1627 ($\nu(\text{C}=\text{N})$, s), 1595 (s), 1532 (s), 1500 (w), 1473 (m), 1453 (s), 1439 (w), 1374 (m), 1344 (s), 1261 (s), 1216 (s), 1153 (w), 1105 (w), 1082 (m), 1030 (s), 999 (w), 957 (m), 906 (s), 870 (s), 799 (s), 778 (s), 748 (s), 707 (s). Anal. Calcd for C₃₆H₃₁Cl₂CoFN₄O₂·(MeOH): C, 60.67; H, 4.82; N, 7.65. Found: C, 60.75; H, 4.40; N, 7.63.

Synthesis of Co^{2Et}. Following the general procedure used for Co^{2Me} synthesis, but with ligand L^{2Et} (0.200 g, 0.33 mmol) and CoCl₂ (0.041 g, 0.31 mmol) instead, a light green Co^{2Et} powder was obtained (0.190 g, Yield: 78%). FTIR (KBr, cm⁻¹): 3086 (w), 3066 (w), 3026 (w), 2968 (m), 1629 ($\nu(\text{C}=\text{N})$, s), 1587 (m), 1524 (s), 1516 (s), 1498 (m), 1465 (m), 1451 (w), 1376 (m), 1335 (s), 1281 (w), 1265 (s), 1216 (m), 1105 (s), 1070 (m), 1032 (w), 961 (w), 872 (w), 803 (s), 770 (m), 748 (s), 705 (s). Anal. Calcd for C₃₈H₃₅Cl₂CoFN₄O₂: C, 62.65; H, 4.84; N, 7.69. Found: C, 62.65; H, 5.03; N, 7.44.

Synthesis of Co^{2iPr}. Following the general procedure used for Co^{2Me} synthesis, but with ligand L^{2iPr} (0.150 g, 0.24 mmol) and CoCl₂ (0.029 g, 0.23 mmol) instead, light green Co^{2iPr} powder was obtained (0.142 g, Yield: 78%). FTIR (KBr, cm⁻¹): 3088 (w), 3062 (w), 2968 (m), 1627 ($\nu(\text{C}=\text{N})$, s), 1589 (m), 1532 (s), 1498 (m), 1469 (w), 1441 (m), 1372 (m), 1346 (s), 1263 (s), 1214 (w), 1206 (w), 1102 (w), 1080 (s), 1028 (m), 999 (w), 955 (w), 914 (w), 876 (m), 815 (m), 801 (s), 770 (m), 748 (s), 707 (s). Anal. Calcd for C₄₀H₃₉Cl₂CoFN₄O₂·(2H₂O): C, 60.61; H, 5.47; N, 7.07. Found: C, 60.42; H, 4.90; N, 6.94.

Synthesis of Co^{3Me}. Following the general procedure used for Co^{2Me} synthesis, but with ligand L^{3Me} (0.150 g, 0.25 mmol) and CoCl₂ (0.031 g, 0.24 mmol) instead, a light green Co^{3Me} powder was obtained (0.143 g, Yield: 78%). FTIR (KBr,

cm⁻¹): 3088 (w), 3029 (w), 2916 (m), 1629 ($\nu(\text{C}=\text{N})$, s), 1593 (m), 1534 (s), 1498 (w), 1453 (w), 1374 (m), 1344 (s), 1263 (s), 1222 (m), 1159 (w), 1078 (m), 1032 (m), 997 (w), 957 (w), 906 (w), 853 (m), 799 (m), 750 (s), 703 (s). Anal. Calcd for C₃₇H₃₃Cl₂CoFN₄O₂·(MeOH): C, 61.14; H, 5.00; N, 7.50. Found: C, 61.29; H, 4.64; N, 7.60.

Synthesis of Co^{2EtMe}. Following the general procedure used for Co^{2Me} synthesis, but with ligand L^{2EtMe} (0.150 g, 0.24 mmol) and CoCl₂ (0.030 g, 0.23 mmol) instead, a light green Co^{2EtMe} powder was obtained (0.140 g, Yield: 77%). FTIR (KBr, cm⁻¹): 3086 (w), 3029 (w), 2968 (m), 1627 ($\nu(\text{C}=\text{N})$, s), 1589 (m), 1530 (s), 1496 (m), 1463 (m), 1372 (m), 1342 (s), 1263 (s), 1218 (m), 1076 (s), 1032 (m), 999 (w), 953 (w), 906 (w), 863 (m), 799 (m), 748 (s), 703 (s). Anal. Calcd for C₃₉H₃₇Cl₂CoFN₄O₂: C, 63.08; H, 5.02; N, 7.55. Found: C, 62.56; H, 5.00; N, 7.45.

■ CONCLUSION

In summary, five new bis(imino)pyridine-cobalt complexes were prepared by incorporating two types of imino units with different steric and electronic substituents and were evaluated for their efficacy in ethylene polymerization. The structures of these complexes were verified by using multiple analytical techniques, including FTIR spectroscopy and X-ray diffraction analysis. Upon in situ activation with either MAO or MMAO, these cobalt complexes demonstrated high efficiency in ethylene polymerization, displaying remarkable activity at 60°C and remained active at elevated temperatures of up to 100°C . The polymers produced had moderate molecular weights, reaching up to 61.0 kg/mol, and displayed unimodal broad dispersity. MAO was found to be a more efficient activator than MMAO for the activation of the cobalt complexes under study. It is revealed that complexes with less steric hindrance showed greater overall activity, while those with more congested structures were better suited for producing high molecular weight polyethylene due to their ability to facilitate chain growth reactions. Moreover, the catalytic activity achieved in this study surpassed that of previously reported bis(imino)pyridylcobalt precatalysts in most cases. The polymerization process predominantly led to chain termination through β -elimination, resulting in α -macroolefins with highly linear long chains. These vinyl-terminated polyethylenes hold significant promise as precursors for the development of new polymers with terminal functional groups, opening avenues for advanced material synthesis and applications.

■ ASSOCIATED CONTENT

Data Availability Statement

The data of this manuscript are available from the corresponding author upon request.

Supporting Information

The Supporting Information is available free of charge at <https://pubs.acs.org/doi/10.1021/prechem.4c00067>.

General consideration, general procedure for ethylene polymerization, X-ray crystallographic studies; crystal data and structural refinements for Co^{2Et} and Co^{2EtMe}, comparison of activity and molecular weight at different Al/Co ratio, and temperatures using MMAO, GPC curves at different Al/Co ratio, and temperatures using MMAO, ¹³C NMR spectra of polyethylene at different conditions, DSC curves of polyethylene at different

temperatures using MAO, FT-IR spectra of Co complexes, references (PDF)

Crystallographic data for Co^{2Et} (CIF)

Crystallographic data for Co^{2EtMe} (CIF)

AUTHOR INFORMATION

Corresponding Authors

Yanping Ma – Key Laboratory of Engineering Plastics and Beijing National Laboratory for Molecular Science, Institute of Chemistry, Chinese Academy of Sciences, Beijing 100190, China; Email: myanping@iccas.ac.cn

Wen-Hua Sun – Key Laboratory of Engineering Plastics and Beijing National Laboratory for Molecular Science, Institute of Chemistry, Chinese Academy of Sciences, Beijing 100190, China; Chemistry and Chemical Engineering Guangdong Laboratory, Shantou 515031, China; CAS Research/Education Center for Excellence in Molecular Sciences and International School, University of Chinese Academy of Sciences, Beijing 100049, China; orcid.org/0000-0002-6614-9284; Email: whsun@iccas.ac.cn

Qaiser Mahmood – Chemistry and Chemical Engineering Guangdong Laboratory, Shantou 515031, China; orcid.org/0000-0002-4160-5108; Email: qaiser@ccelab.com.cn

Authors

Kainat Fatima Tahir – Key Laboratory of Engineering Plastics and Beijing National Laboratory for Molecular Science, Institute of Chemistry, Chinese Academy of Sciences, Beijing 100190, China; Chemistry and Chemical Engineering Guangdong Laboratory, Shantou 515031, China; CAS Research/Education Center for Excellence in Molecular Sciences and International School, University of Chinese Academy of Sciences, Beijing 100049, China

Geng Ren – Chemistry and Chemical Engineering Guangdong Laboratory, Shantou 515031, China

Areej Khalid – Key Laboratory of Engineering Plastics and Beijing National Laboratory for Molecular Science, Institute of Chemistry, Chinese Academy of Sciences, Beijing 100190, China; Chemistry and Chemical Engineering Guangdong Laboratory, Shantou 515031, China; CAS Research/Education Center for Excellence in Molecular Sciences and International School, University of Chinese Academy of Sciences, Beijing 100049, China

Yizhou Wang – Key Laboratory of Engineering Plastics and Beijing National Laboratory for Molecular Science, Institute of Chemistry, Chinese Academy of Sciences, Beijing 100190, China; CAS Research/Education Center for Excellence in Molecular Sciences and International School, University of Chinese Academy of Sciences, Beijing 100049, China

Song Zou – Key Laboratory of Engineering Plastics and Beijing National Laboratory for Molecular Science, Institute of Chemistry, Chinese Academy of Sciences, Beijing 100190, China

Tongling Liang – CAS Research/Education Center for Excellence in Molecular Sciences and International School, University of Chinese Academy of Sciences, Beijing 100049, China

Complete contact information is available at:
<https://pubs.acs.org/10.1021/prechem.4c00067>

Notes

The authors declare no competing financial interest.

ACKNOWLEDGMENTS

This work has been financially supported by the Chemistry and Chemical Engineering Guangdong Laboratory (2111018 and 2132012). K.F.T. would like to express gratitude towards the ANSO Scholarship Program for their support.

REFERENCES

- (1) Àngeles Cartes, M.; Rodríguez-Delgado, A.; Palma, P.; Sánchez, L. J.; Cámpora, J. Direct evidence for a coordination–insertion mechanism of ethylene oligomerization catalysed by neutral 2,6-bis(imino)pyridine iron monoalkyl complexes. *Catal. Sci. Technol.* **2014**, *4* (8), 2504–2507.
- (2) Tomov, A. K.; Gibson, V. C.; Britovsek, G. J. P.; Long, R. J.; Meurs, M. V.; Jones, D. J.; Tellmann, K. P.; Chirinos, J. J. Distinguishing chain growth mechanisms in metal-catalyzed olefin oligomerization and polymerization systems: C₂H₄/C₂D₄ co-oligomerization/polymerization experiments using chromium, iron, and cobalt catalysts. *Organometallics* **2009**, *28* (24), 7033–7040.
- (3) Cossee, P. Ziegler-Natta catalysis I. mechanism of polymerization of α -olefins with Ziegler-Natta catalysts. *J. Catal.* **1964**, *3* (1), 80–88.
- (4) Umare, P. S.; Rao, K.; Tembe, G. L.; Dhoble, D. A.; Trivedi, B. Controlled synthesis of low-molecular-weight polyethylene waxes by titanium–biphenolate–ethylaluminum sesquichloride based catalyst systems. *J. Appl. Polym. Sci.* **2007**, *104*, 1531–1539.
- (5) Patel, K.; Chikkali, S. H.; Sivaram, S. Ultrahigh molecular weight polyethylene: Catalysis, structure, properties, processing and applications Ultrahigh molecular weight polyethylene: Catalysis, structure, properties, processing and applications. *Prog. Polym. Sci.* **2020**, *109*, 101290.
- (6) Dashti, A.; Ahmadi, M. Recent Advances in Controlled Production of Long-Chain Branched Polyolefins. *Macromol. Rapid Commun.* **2024**, *45*, 2300746.
- (7) Alzamy, A.; Bakiro, M.; Ahmed, S. H.; Siddig, L. A.; Nguyen, H. L. Linear α -olefin oligomerization and polymerization catalyzed by metal-organic frameworks. *Coord. Chem. Rev.* **2022**, *462*, 214522.
- (8) Houst, Y. F.; Bowen, P.; Perche, F.; Kauppi, A.; Borget, P.; Galmiche, L.; Le Meins, J. F.; Lafuma, F.; Flatt, R. J.; Schober, I.; et al. Design and function of novel superplasticizers for more durable high-performance concrete (Superplast project). *Cem. Concr. Res.* **2008**, *38* (10), 1197–1209.
- (9) Richard, T. L. In *Global Legislation for Food Contact Materials*, Second ed.; 2022. DOI: [10.1016/C2019-0-02194-2](https://doi.org/10.1016/C2019-0-02194-2).
- (10) Golub, F. S.; Bolotov, V. A.; Parmon, V. N. Current Trends in the Processing of Linear Alpha Olefins into Technologically Important Products: Part 2. *Catal. Ind.* **2021**, *13*, 203–215.
- (11) Shokri, A.; Karimi, S. A Review in Linear Alkylbenzene (LAB) Production Processes in the Petrochemical Industry. *Russ. J. Appl. Chem.* **2021**, *94*, 1546–1559.
- (12) Gibson, V. C.; Solan, G. A. Iron-based and cobalt-based olefin polymerisation catalysts. *Top. Organometal. Chem.* **2009**, *26*, 107–158.
- (13) Gibson, V. C.; Solan, G. A. Olefin oligomerizations and polymerizations catalyzed by iron and cobalt complexes bearing bis(imino)pyridine ligands. *Catalysis Without Precious Metals.* **2010**, 111–141.
- (14) Small, B. L.; Brookhart, M. Iron-based catalysts with exceptionally high activities and selectivities for oligomerization of ethylene to linear α -olefins. *J. Am. Chem. Soc.* **1998**, *120*, 7143–7144.
- (15) Busico, V.; Cipullo, R.; Chadwick, J. C.; Modder, J. F.; Sudmeijer, O. Effects of regiochemical and stereochemical errors on the course of isotactic propene polyinsertion promoted by homogeneous Ziegler-Natta catalysts. *Macromolecules* **1994**, *27*, 7538–7543.

- (16) Bochmann, M.; Lancaster, S. J. Monomer–dimer equilibria in homo- and heterodinuclear cationic alkylzirconium complexes and their role in polymerization catalysis. *Angew. Chem. Int. Ed.* **1994**, *33* (15–16), 1634–1637.
- (17) Zambelli, A.; Longo, P.; Grassi, A. Isotactic polymerization of propene: homogeneous catalysts based on group 4 metallocenes without methylalumoxane. *Macromolecules.* **1989**, *22* (5), 2186–2189.
- (18) Marques, M. M. V.; Nunes, C. P.; Tait, P. J. T.; Dias, A. R. Polymerization of ethylene using a high-activity Ziegler–Natta catalyst. II. Molecular weight regulation. *J. Polym. Sci. Part A Polym. Chem.* **1993**, *31* (1), 219–225.
- (19) (a) Guan, Z.; Cotts, P. M.; McCord, E. F.; McLain, S. J. Chain Walking: A New Strategy to Control Polymer Topology. *Science* **1999**, *283*, 2059–2062. (b) Mahmood, Q.; Sun, W. H. N-chelated nickel catalysts for highly branched polyolefin elastomers: a survey. *R. Soc. Open.* **2018**, *5*, 180367. (c) Mahmood, Q.; Li, X.; Qin, L.; Wang, L.; Sun, W. H. Structural evolution of iminopyridine support for nickel/palladium catalysts in ethylene (oligo)polymerization. *Dalton Trans.* **2022**, *51*, 14375. (d) Saeed, H.; Mahmood, Q.; Yuan, R.; Wang, Y.; Zou, S.; Tahir, K. F.; Ma, Y.; Liang, T.; Sun, W. H. High-performance polyethylene elastomers using a hybrid steric approach in α -diimine nickel precatalysts. *Polym. Chem.* **2024**, *15*, 1437. (e) Hu, Z.; Ren, G.; Mahmood, Q.; Yu, Z.; Wang, Y.; Tahir, K. F.; Zou, S.; Liang, T.; Sun, W. H. Thermostability promotion of α -diimine nickel precatalysts tailored with 2,6-bis(bis(4-fluorophenyl)methyl)-3,4,5-trimethoxyaniline for PE elastomer synthesis. *New J. Chem.* **2024**, *48*, 12174–12187. (f) Wang, L.; Liu, M.; Mahmood, Q.; Yuan, S.; Li, X.; Qin, L.; Zou, S.; Liang, T.; Sun, W. H. Enhancing the thermal stability of α -Diimine Ni(II) catalysts for ethylene polymerization via symmetrical axial shielding strategy. *Eur. Polym. J.* **2023**, *194*, 112112.
- (20) (a) Britovsek, G. J. P.; Bruce, M.; Gibson, V. C.; Kimberley, B. S.; Maddox, P. J.; Mastroianni, S.; McTavish, S. J.; Redshaw, C.; Solan, G. A.; Strömberg, S.; White, A. J. P.; Williams, D. J. Iron and cobalt ethylene polymerization catalysts bearing 2,6-bis(imino)pyridyl ligands: synthesis, structures, and polymerization studies. *J. Am. Chem. Soc.* **1999**, *121*, 8728–8740. (b) Wang, Z.; Mahmood, Q.; Zhang, W.; Sun, W. H. Recent progress on the tridentate iron complex catalysts for ethylene oligo-/polymerization. *Adv. Organomet. Chem.* **2023**, *79*, 41–86. (c) Mahmood, Q.; Yue, E.; Guo, J.; Zhang, W.; Ma, Y.; Hao, X.; Sun, W. H. Nitrofunctionalized bis(imino)pyridylferrous chlorides as thermo-stable precatalysts for linear polyethylenes with high molecular weights. *Polymer.* **2018**, *159*, 124–137. (d) Sage, D. D.; Zhang, Q.; Mahmood, Q.; Ma, Y.; Liu, M.; Hao, X.; Sun, W. H. Nitro and 4,4'-fluorobenzhydryl functionalized bis(imino)pyridine-cobalt complexes for high molecular weight linear polyethylenes. *Polymer.* **2023**, *285*, 126384.
- (21) Small, B. L.; Brookhart, M.; Bennett, A. M. A. Highly active iron and cobalt catalysts for the polymerization of ethylene. *J. Am. Chem. Soc.* **1998**, *120*, 4049–4050.
- (22) Britovsek, G. J. P.; Gibson, V. C.; Kimberley, B. S.; Maddox, P. J.; McTavish, S. J.; Solan, G. A.; White, A. J. P.; Williams, D. J. Novel olefin polymerization catalysts based on iron and cobalt. *Chem. Commun.* **1998**, *8*, 849–850.
- (23) Guan, Z.; Popeney, C. S. Recent Progress in Late Transition Metal α -Diimine Catalysts for Olefin Polymerization. In: *Metal Catalysts in Olefin Polymerization*; Guan, Z., Ed.; Topics in Organometallic Chemistry, 2009; Vol. 26.
- (24) Sun, W. H.; Jie, S.; Zhang, S.; Zhang, W.; Song, Y.; Ma, H.; et al. Iron complexes bearing 2-imino-1,10-phenanthroline ligands as highly active catalysts for ethylene oligomerization. *Organometallics.* **2006**, *25*, 666–677.
- (25) Sun, W. H.; Hao, P.; Zhang, S.; Shi, Q.; Zuo, W.; Tang, X.; et al. Iron(II) and Cobalt(II) 2-(Benzimidazolyl)-6-(1-(arylimino)-ethyl)pyridyl Complexes as Catalysts for Ethylene Oligomerization and Polymerization. *Organometallics.* **2007**, *26*, 2720–2734.
- (26) Pelascini, F.; Wesolek, M.; Peruch, F.; Lutz, P. J. Modified Pyridine-Bis(imine) Iron and Cobalt Complexes: Synthesis, Structure, and Ethylene Polymerization Study. *Eur. J. Inorg. Chem.* **2006**, *2006*, 4309–4316.
- (27) (a) Jie, S.; Zhang, S.; Wedeking, K.; Zhang, W.; Ma, H.; Lu, X.; Deng, Y.; Sun, W. H. Cobalt(II) complexes bearing 2-imino-1,10-phenanthroline ligands: synthesis, characterization and ethylene oligomerization. *C. R. Chimie.* **2006**, *9*, 1500–1509. (b) Pelletier, J. D.A.; Champouret, Y. D. M.; Cadarso, J.; Clowes, L.; Gañete, M.; Singh, K.; Thanarajasingham, V.; Solan, G. A. Electronically variable imino-phenanthroline-cobalt complexes; synthesis, structures and ethylene oligomerisation studies. *J. Organomet. Chem.* **2006**, *691* (19), 4114–4123.
- (28) (a) Gao, R.; Wang, K.; Li, Y.; Wang, F.; Sun, W. H.; Redshaw, C.; Bochmann, M. 2-Benzoxazolyl-6-(1-(arylimino)ethyl)pyridyl cobalt (II) chlorides: A temperature switch catalyst in oligomerization and polymerization of ethylene. *J. Mol. Catal. A: Chem.* **2009**, *309*, 166–171. (b) Han, M.; Zhang, Q.; Oleynik, I. I.; Suo, H.; Solan, G. A.; Oleynik, I. V.; Ma, Y.; Liang, T.; Sun, W. H. High molecular weight polyethylenes of narrow dispersity promoted using bis(arylimino)cyclohepta[b]pyridine-cobalt catalysts ortho-substituted with benzhydryl & cycloalkyl groups. *Dalton Trans.* **2020**, *49*, 4774–4784. (c) Ba, J.; Du, S.; Yue, E.; Hu, X.; Flisak, Z.; Sun, W. H. Constrained formation of 2-(1-(arylimino)ethyl)-7-arylimino-6,6-dimethylcyclopentapyridines and their cobalt(II) chloride complexes: synthesis, characterization and ethylene polymerization. *RSC Adv.* **2015**, *5*, 32720. (d) Suo, H.; Oleynik, I. V.; Oleynik, I. I.; Solan, G. A.; Ma, Y.; Liang, T.; Sun, W. H. Post-functionalization of narrowly dispersed PE waxes generated using tuned N,N,N'-cobalt ethylene polymerization catalysts substituted with ortho-cycloalkyl groups. *Polymer* **2021**, *213*, 123294. (e) Huang, F.; Zhang, W.; Yue, E.; Liang, T.; Hu, X.; Sun, W. H. Controlling the molecular weights of polyethylene waxes using the highly active precatalysts of 2-(1-(arylimino)ethyl)-9-arylimino-5,6,7,8-tetrahydrocycloheptapyridylcobalt chlorides: synthesis, characterization, and catalytic behavior. *Dalton Trans.* **2016**, *45* (2), 657–666. (f) Huang, F.; Zhang, W.; Sun, Y.; Hu, X.; Solan, G. A.; Sun, W. H. Thermally stable and highly active cobalt precatalysts for vinyl-polyethylenes with narrow polydispersities: integrating fused-ring and imino-carbon protection into ligand design. *New J. Chem.* **2016**, *40* (9), 8012–8023. (g) Sun, W. H.; Kong, S.; Chai, W.; Shiono, T.; Redshaw, C.; Hu, X.; Guo, C.; Hao, X. 2-(1-(Arylimino)ethyl)-8-arylimino-5,6,7-trihydroquinolylcobalt dichloride: Synthesis and polyethylene wax formation. *Appl. Catal.* **2012**, *447–448*, 67–73.
- (29) Appukuttan, V. K.; Liu, Y.; Son, B. C.; Ha, C. S.; Suh, H.; Kim, I. Iron and Cobalt Complexes of 2,3,7,8-Tetrahydroacridine-4,5-(1H,6H)-diimine Sterically Modulated by Substituted Aryl Rings for the Selective Oligomerization to Polymerization of Ethylene. *Organometallics.* **2011**, *30*, 2285–2294.
- (30) (a) Bariashir, C.; Wang, Z.; Suo, H.; Zada, M.; Solan, G. A.; Ma, Y.; Liang, T.; Sun, W. H. Narrow dispersed linear polyethylene using cobalt catalysts bearing cycloheptyl-fused bis(imino)pyridines; probing the effects of orthobenzhydryl substitution. *Eur. Polym. J.* **2019**, *110*, 240–251. (b) Suo, H.; Oleynik, I. I.; Bariashir, C.; Oleynik, I. V.; Wang, Z.; Solan, G. A.; Ma, Y.; Liang, T.; Sun, W. H. Strictly linear polyethylene using Co-catalysts chelated by fused bis(arylimino)pyridines: Probing ortho-cycloalkyl ring-size effects on molecular weight. *Polymer.* **2018**, *149*, 45–54. (c) Wang, Z.; Solan, G. A.; Mahmood, Q.; Liu, Q.; Ma, Y.; Hao, X.; Sun, W. H. Bis(imino)pyridines Incorporating Doubly Fused Eight-Membered Rings as Conformationally Flexible Supports for Cobalt Ethylene Polymerization Catalysts. *Organometallics.* **2018**, *37*, 380–389. (d) Zada, M.; Guo, L.; Zhang, W.; Ma, Y.; Liang, T.; Sun, W. H. Rational Design of Cycloheptyl-Fused Bis(arylimino)pyridylcobalt(II) Precatalysts Adorned with Sterically and Electronically Modified N-Aryls for Enhancing Ethylene Polymerization. *Eur. J. Inorg. Chem.* **2021**, *2021*, 720–733. (e) Zhang, Q.; Wu, N.; Xiang, J.; Solan, G. A.; Suo, H.; Ma, Y.; Liang, T.; Sun, W. H. Bis-cycloheptyl-fused bis(imino)pyridine-cobalt catalysts for PE wax formation: positive effects of fluoride substitution on catalytic performance and thermal stability. *Dalton Trans.* **2020**, *49*, 9425–9437. (f) Wang, Z.; Ma, Y.; Guo, J.; Liu, Q.; Solan, G. A.; Liang, T.; Sun, W. H. Bis(imino)pyridines fused with 6- and 7-membered carbocyclic rings as N,N,N-

- scaffolds for cobalt ethylene polymerization catalysts. *Dalton Trans.* **2019**, 48, 2582–2591. (g) Wang, Y.; Wang, Z.; Zhang, Q.; Zou, S.; Ma, Y.; Solan, G. A.; Zhang, W.; Sun, W. H. Exploring Long Range para-Phenyl Effects in Unsymmetrically Fused bis(imino)pyridine-Cobalt Ethylene Polymerization Catalysts. *Catalysts*. **2023**, 13 (10), 1387.
- (31) Wang, S.; Li, B.; Liang, T.; Redshaw, C.; Li, Y.; Sun, W. H. Synthesis, characterization and catalytic behavior toward ethylene of 2-[1-(4,6-dimethyl-2-benzhydrylphenylimino)ethyl]-6-[1-(arylimino)ethyl]-pyridylmetal(iron or cobalt) chlorides. *Dalton Trans.* **2013**, 42, 9188.
- (32) Lai, J.; Zhao, W.; Yang, W.; Redshaw, C.; Liang, T.; Liu, Y.; Sun, W. H. 2-[1-(2,4-Dibenzhydryl-6-methylphenylimino)ethyl]-6-[1-(arylimino)ethyl] pyridylcobalt(II) dichlorides: Synthesis, characterization and ethylenepolymerization behavior. *Polym. Chem.* **2012**, 3, 787.
- (33) Zhang, W.; Wang, S.; Du, S.; Guo, C. Y.; Hao, X.; Sun, W. H. 2-(1-(2,4-Bis((di(4-fluorophenyl)methyl)-6-methylphenylimino)ethyl)-6-(1-(arylimino)ethyl)pyridylmetal (iron or cobalt) Complexes: Synthesis, Characterization, and Ethylene Polymerization Behavior. *Macromol. Chem. Phys.* **2014**, 215, 1797–1809.
- (34) Yuan, S. F.; Fan, Z.; Yan, Y.; Ma, Y.; Han, M.; Liang, T.; Sun, W. H. Achieving polydispersive HDPE by N,N,N-Co precatalysts appended with N-2,4-bis(di(4-methoxyphenyl)methyl)-6-methylphenyl. *RSC Adv.* **2020**, 10, 43400.
- (35) Bariashir, C.; Zhang, R.; Vignesh, A.; Ma, Y.; Liang, T.; Sun, W. H. Enhancing Ethylene Polymerization of NNN-Cobalt(II) Precatalysts Adorned with a Fluoro-substituent. *ACS Omega*. **2021**, 6, 4448–4460.
- (36) Zhang, Q.; Li, Z.; Han, M.; Xiang, J.; Solan, G. A.; Ma, Y.; Liang, T.; Sun, W. H. Fluorinated cobalt catalysts and their use in forming narrowly dispersed polyethylene waxes of high linearity and incorporating vinyl functionality. *Catal. Sci. Technol.* **2021**, 11, 656.
- (37) Han, M.; Oleynik, I. I.; Liu, M.; Ma, Y.; Oleynik, I. V.; Solan, G. A.; Liang, T.; Sun, W. H. Ring size enlargement in an ortho-cycloalkyl-substituted bis(imino)pyridine-cobalt ethylene polymerization catalyst and its impact on performance and polymer properties. *Appl. Organomet. Chem.* **2022**, 36, No. e6529.
- (38) Yu, J.; Huang, W.; Wang, L.; Redshaw, C.; Sun, W. H. 2-[1-(2,6-Dibenzhydryl-4-methylphenylimino)ethyl]-6-[1-(arylimino)ethyl]pyridylcobalt(II) dichlorides: Synthesis, characterization and ethylene polymerization behavior. *Dalton Trans.* **2011**, 40, 10209–10214.
- (39) Wang, S.; Zhao, W.; Hao, X.; Li, B.; Redshaw, C.; Li, Y.; Sun, W. H. 2-(1-{2,6-Bis[bis(4-fluorophenyl)methyl]-4-methylphenylimino}ethyl)-6-[1-(arylimino)ethyl]pyridylcobalt dichlorides: Synthesis, characterization and ethylene polymerization behavior. *J. Organomet. Chem.* **2013**, 731, 78–84.
- (40) Liu, T.; Liu, M.; Ma, Y.; Solan, G. A.; Liang, T.; Sun, W. H. Cobalt Catalysts Bearing ortho-(4,4'-Dichlorobenzhydryl) Substituents and Their Use in Generating Narrowly Dispersed Polyethylene of High Linearity. *Eur. J. Inorg. Chem.* **2022**, 2022, No. e202200396.
- (41) Yuan, S. F.; Wang, L.; Yan, Y.; Liu, T.; Flisak, Z.; Ma, Y.; Sun, W. H. 4,4-Dimethoxybenzhydryl substituent augments performance of bis(imino)pyridine cobalt-based catalysts in ethylene polymerization. *RSC Adv.* **2022**, 12, 15741.
- (42) Zhang, Q.; Ma, Y.; Suo, H.; Solan, G. A.; Liang, T.; Sun, W. H. Co-catalyst effects on the thermal stability/activity of N,N,N-Co ethylene polymerization Catalysts Bearing Fluoro-Substituted N-2,6-dibenzhydrylphenyl groups. *Appl. Organomet. Chem.* **2019**, 33, No. e5134.
- (43) He, F.; Zhao, W.; Cao, X. P.; Liang, T.; Redshaw, C.; Sun, W. H. 2-[1-(2,6-dibenzhydryl-4-chlorophenylimino)ethyl]-6-[1-(arylimino)ethyl]pyridyl cobalt dichlorides: Synthesis, characterization and ethylene polymerization behavior. *J. Organomet. Chem.* **2012**, 713, 209–216.
- (44) Mahmood, Q.; Ma, Y.; Hao, X.; Sun, W. H. Substantially enhancing the catalytic performance of bis(imino)pyridylcobaltous chloride pre-catalysts adorned with benzhydryl and nitro groups for ethylene Polymerization. *Appl. Organomet. Chem.* **2019**, 33, No. e4857.
- (45) Zhang, R.; Ma, Y.; Han, M.; Solan, G. A.; Pi, Y.; Sun, Y.; Sun, W. H. Exceptionally high molecular weight linear polyethylene by using N,N,N'-Co catalysts appended with a N'-2,6-bis(di(4-fluorophenyl)methyl)-4-nitrophenyl group. *Appl. Organomet. Chem.* **2019**, 33, No. e5157.
- (46) Yan, Y.; Yuan, S. F.; Liu, M.; Solan, G. A.; Ma, Y.; Liang, T.; Sun, W. H. Investigating the Effects of Para-methoxy Substitution in Sterically Enhanced Unsymmetrical Bis(arylimino)pyridine-cobalt Ethylene Polymerization Catalysts. *Chin. J. Polym. Sci.* **2022**, 40, 266–279.
- (47) Liu, M.; Jiang, S.; Ma, Y.; Solan, G. A.; Sun, Y.; Sun, W. H. CF₃O-Functionalized Bis(arylimino)pyridine-Cobalt Ethylene Polymerization Catalysts: Harnessing Solvent Effects on Performance and Polymer Properties. *Organometallics*. **2022**, 41, 3237–3248.
- (48) Tahir, K. F.; Ma, Y.; Mahmood, Q.; Wang, Y.; Ren, G.; Zou, S.; Saeed, H.; Liang, T.; Sun, W. H. Bis(imino)pyridyliron incorporated with NO₂, F and benzhydryl substituents as thermostable precatalysts for vinyl-terminated polyethylenes. *Polymer*. **2024**, 308, 127335.
- (49) Crans, D. C.; Tarlton, M. L.; McLauchlan, C. C. Trigonal bipyramidal or square pyramidal coordination geometry? Investigating the most potent geometry for vanadium phosphatase inhibitors. *Eur. J. Inorg. Chem.* **2014**, 2014, 4450–4468.
- (50) Zhang, W.; Sun, W. H.; Redshaw, C. Tailoring iron complexes for ethylene oligomerization and/or polymerization. *Dalton Trans.* **2013**, 42 (25), 8988–8997.
- (51) Britovsek, G. J. P.; Gibson, V. C.; Kimberley, B. S.; Mastroianni, S.; Redshaw, C.; Solan, G. A.; White, A. J. P.; Williams, D. J. Bis(imino)pyridyl iron and cobalt complexes: the effect of nitrogen substituents on ethylene oligomerization and polymerization. *J. Chem. Soc., Dalton Trans.* **2001**, 1639–1644.
- (52) Lee, L. S.; Ou, H. J.; Hsu, H. F. The experiments and correlations of the solubility of ethylene in toluene solvent. *Fluid Phase Equilib.* **2005**, 231, 221–230.
- (53) Svejda, S. A.; Johnson, K. L.; Brookhart, M. Low-temperature spectroscopic observation of chain growth and migratory insertion barriers in (α -Diimine)Ni(II) olefin polymerization catalysts. *J. Am. Chem. Soc.* **1999**, 121, 10634.
- (54) Makio, H.; Terao, H.; Iwashita, A.; Fujita, T. FI catalysts for olefin polymerization—a comprehensive treatment. *Chem. Rev.* **2011**, 111, 2363–2449.
- (55) De Souza, C. G.; de Souza, R. F.; Bernardo-Gusmão, K. Effect of alkylaluminum cocatalyst on ethylene polymerization with nickel- α -diimine complex. *Appl. Catal.* **2007**, 325, 87–90.
- (56) Simon, L. C.; Mauler, R. S.; De Souza, R. F. Effect of the alkylaluminum cocatalyst on ethylene polymerization by a nickel-diimine complex. *J. Polym. Sci., Part A: Polym. Chem.* **1999**, 37, 4656–4663.
- (57) (a) Mahmood, Q.; Guo, J.; Zhang, W.; Ma, Y.; Liang, T.; Sun, W. H. Concurrently improving the thermal stability and activity of ferrous precatalysts for the production of saturated/unsaturated polyethylene. *Organometallics* **2018**, 37, 957–970. (b) Huang, C.; Vignesh, A.; Bariashir, C.; Mahmood, Q.; Ma, Y.; Sun, Y.; Sun, W. H. Producing highly linear polyethylenes by using t-butyl-functionalized 2,6-bis(imino)pyridylchromium(III) chlorides. *J. Polym. Sci., Part A: Polym. Chem.* **2019**, 57 (10), 1049–1058.
- (58) Han, M.; Zuo, Z.; Ma, Y.; Solan, G. A.; Hu, X.; Liang, T.; Sun, W. H. Bis(imino)-6,7-dihydro-5H-quinoline-cobalt complexes as highly active catalysts for the formation of vinyl-terminated PE waxes; steps towards inhibiting deactivation pathways through targeted ligand design. *RSC Adv.* **2021**, 11, 39869–39878.
- (59) Bocian, A.; Skrodzki, M.; Kubicki, M.; Gorczyński, A.; Pawluć, P.; Patroniak, V. The effect of Schiff base ligands on the structure and catalytic activity of cobalt complexes in hydrosilylation of olefins. *Appl. Catal.* **2020**, 602, 117665.
- (60) Falivene, L.; Credendino, R.; Poater, A.; Petta, A.; Serra, L.; Oliva, R.; Scarano, V.; Cavallo, L. SambVca2. A Web Tool for

Analyzing Catalytic Pockets with Topographic Steric Maps. *Organometallics*. **2016**, 35, 2286–2293.

(61) Takeuchi, D.; Takano, S.; Takeuchi, Y.; Osakada, K. Ethylene Polymerization at High Temperatures Catalyzed by DoubleDecker-Type Dinuclear Iron and Cobalt Complexes: Dimer Effect on Stability of the Catalyst and Polydispersity of the Product. *Organometallics*. **2014**, 33, 5316–5323.